Ab Initio No Core Shell Model — Recent Results and Further Prospects

James P. Vary[a], Pieter Maris[a], Hugh Potter[a],
Mark A. Caprio[b], Robin Smith[c], Sven Binder[d,e], Angelo Calci[f],
Sebastian Fischer[g], Joachim Langhammer[g], Robert Roth[g],
Hasan Metin Aktulga[h,i] Esmond Ng[i], Chao Yang[i],
Dossay Oryspayev[j], Masha Sosonkina[k], Erik Saule[l]
and Ümit Çatalyürek[m,n].

[a] *Department of Physics and Astronomy, Iowa State University, Ames, IA 50011, USA*

[b] *Department of Physics, University of Notre Dame, Notre Dame, IN 46556, USA*

[c] *School of Physics and Astronomy, University of Birmingham, Birmingham B15 2TT, UK*

[d] *Department of Physics and Astronomy, University of Tennessee, Knoxville, TN 37996, USA*

[e] *Physics Division, Oak Ridge National Laboratory, Oak Ridge, TN 37831, USA*

[f] *TRIUMF, 4004 Wesbrook Mall, Vancouver, British Columbia, V6T 2A3, Canada*

[g] *Institut für Kernphysik, Technische Universität Darmstadt, 64289 Darmstadt, Germany*

[h] *Department of Computer Science, Michigan State University, East Lansing, MI 48844, USA*

[i] *Lawrence Berkeley National Laboratory, Berkeley, CA 94720, USA*

[j] *Department of Electrical and Computer Engineering, Iowa State University, Ames, IA 50011, USA*

[k] *Department of Modeling, Simulation and Visualization Engineering, Old Dominion University, Norfolk, VA 23529, USA*

[l] *Department of Computer Science, University of North Carolina Charlotte, Charlotte, NC 28223, USA*

[m] *Department of Biomedical Informatics, The Ohio State University, Columbus, OH 43210, USA*

[n] *Department of Electrical and Computer Engineering, The Ohio State University, Columbus, OH 43210, USA*

Abstract

There has been significant recent progress in solving the long-standing problems of how nuclear shell structure and collective motion emerge from underlying microscopic inter-nucleon interactions. We review a selection of recent significant results within the *ab initio* No Core Shell Model (NCSM) closely tied to three major factors enabling this progress: (1) improved nuclear interactions that accurately describe the experimental two-nucleon and three-nucleon interaction data; (2) advances in algorithms to simulate the quantum many-body problem with strong interactions; and (3) continued rapid development of high-performance computers now capable of performing 20×10^{15} floating point operations per second. We also comment on prospects for further developments.

Keywords: *No Core Shell Model; chiral Hamiltonians; JISP16; petascale computers; exascale computers*

1   Introduction

The *ab initio* No Core Shell Model (NCSM), using realistic microscopic nucleon-nucleon (NN) and three-nucleon forces (3NFs), has proven to be a powerful combination for describing and predicting properties of light nuclei [1–7]. The Hamiltonian framework results in a large sparse matrix eigenvalue problem for which we seek the low-lying eigenvalues and eigenvectors to form comparisons with experimental data and to make testable predictions. Given the rapid advances in hardware with frequent disruptions in architecture, it has become essential for physicists, computer scientists and applied mathematicians to work in close collaboration in order to achieve efficient solutions to forefront physics problems. Fortunately, US funding agencies have recognized these challenges at the interface of science and technology and have provided support leading to our recent successes [8–17].

We present here a selection of recent results for light nuclei and neutron drops in external traps and set out some of the challenges that lie ahead. The results include both those utilizing the JISP16 NN interaction and those using chiral effective field theory NN plus 3N interactions. We also present a selection of algorithms developed for high-performance computers that are helping to rapidly pave the way to efficient utilization of exascale machines (10^{18} floating point operations per second). We illustrate the scientific progress attained with multi-disciplinary teams of physicists, computer scientists and applied mathematicians.

This paper is aimed to complement presentations at this meeting that cover closely-related topics. In this connection, it is important to point especially to the papers by Dytrych *et al.* [18], by Abe *et al.* [19], by Shirokov *et al.* [20] and by Mazur *et al.* [21]. We therefore focus here on the following recent results: (1) demonstrating the emergence of collective rotations in light nuclei; (2) achieving an accurate description of the properties of ^{12}C with chiral Hamiltonians; (3) solving for properties of neutron drops with chiral Hamiltonians; (4) development of techniques for efficient use of computational accelerators; and (5) development of techniques for overlapping communication and computation.

2   Emergence of collective rotations

NCSM calculations of various types have been used to demonstrate the emergence of collective rotational correlations in p-shell nuclei, including ^{6}Li [18, 22], the Be isotopes [22–25], and ^{12}C [26]. Here we focus on the results for the Be isotopes solved in the No Core Full Configuration (NCFC) framework [4,6,7] using the realistic JISP16 NN interaction [27, 28] with the M-scheme harmonic oscillator (HO) basis. The NCFC framework uses many of the same techniques as the NCSM but additionally features extrapolations of observables to the infinite matrix limit [4].

With no prior selection of our basis to favor solutions with collective motion and using only the realistic bare NN interaction (i. e. we omit the Coulomb interaction to ensure exact conservation of isospin thereby simplifying the spectrum[1]) we face the task of analyzing our microscopic results and determining which particular states, among the large number of calculated levels, exhibit signatures of collective nuclear motion. We follow the path of calculating observables and post-analyzing their systematics to infer that they follow the patterns prescribed by collective rotation. This path is analogous to that taken when analyzing experimental data. When we discover patterns appropriate to a collective band in our calculated results, we assign the moniker of "collective motion" to our microscopic results. We further compare the so-detected band with experimental results and find good agreement which fur-

---

[1]The primary effect of the Coulomb is to shift the binding energies which would not affect our analysis of rotational band observables. New analysis including Coulomb [29] confirms this.

ther supports our discovery of emergent collective phenomena in light nuclei from the underlying microscopic many-body theory.

The details of this step-by-step analysis may be found in the Refs. [23–25]. We analyze the systematics of calculated excitation energies, quadrupole moments, dipole moments, electric quadrupole transition $B(E2)$'s and their reduced matrix elements to isolate states which have a clear rotation band assignment from those which do not. In this way, we have identified both ground state and excited state bands, both natural and unnatural parity bands, and bands in even-even as well as in even-odd nuclei.

Perhaps the most striking hallmark of collective rotation is the appearance of excited states with excitation energies that follow a simple pattern prescribed by the collective model. This pattern of collective rotational excitation energies is given in Eq. (1):

$$E(J) = E_0 + A\big[J(J+1) + a(-)^{J+1/2}(J+\tfrac{1}{2})\delta_{K,1/2}\big], \tag{1}$$

where E_0 is an offset to properly position excited band heads relative to the lowest band head, a is the Coriolis decoupling parameter for $K = \frac{1}{2}$ bands appearing in odd-A nuclei, J is the total angular momentum and $A \equiv \hbar^2/(2\mathcal{J})$ with $\mathcal{J}$ representing the moment of inertia of the deformed nucleus.

To be convinced that the states are indeed members of a rotational band one needs to find that these states also exhibit enhanced electromagnetic moments and transition rates that exhibit a dependence on angular momentum J that is also prescribed by the collective rotational model. We therefore adopt these additional criteria for assigning calculated states to rotational bands. It is worth noting here that, in light nuclei, gamma decay data are scarce due to the short-lived resonant nature of the states. Therefore, the calculations provide access to quantities that are typically inaccessible in experiment, yet crucial for confirming collectivity.

We extract parameters of the traditional rotational description through fits to our theoretical results after extrapolation to the the infinite matrix limit (for extrapolation details see Ref. [25]) and we compare these extracted parameters with rotational parameters determined from similar fits to the corresponding experimental data. The energy parameters for bands across the Be isotopic chain are summarized in Fig. 1: the band excitation energy E_x (defined relative to the yrast band as $E_x \equiv E_0 - E_{0,\mathrm{yrast}}$), the band rotational parameter or slope A, and the band Coriolis decoupling parameter or staggering a (for $K = 1/2$).

In total, we compare 23 theoretical and experimental collective rotation parameters for energies in the 6 Be isotopes depicted in Fig. 1. Overall the agreement between theory and experiment is remarkable. Additional analyses of the calculated electromagnetic observables in Refs. [23–25] and comparison with sparse data available confirm that we have observed the emergent phenomena of collective rotation in these *ab initio* calculations for the Be isotopes. At the same time, there are opportunities for additional theoretical and experimental research to explore, for example, where rotational bands terminate and whether additional bands may be found in these and other light nuclei. It appears that bands do not always terminate at the state corresponding to the maximum angular momentum supported by the nucleons occupying the standard valence shell model orbitals [23–25].

3 Chiral Hamiltonian description of ^{12}C

Recent significant theoretical advances for the underlying Hamiltonians, constructed within chiral effective field theory (EFT), provide a foundation for nuclear many-body calculations rooted in QCD [30,31]. These developments motivate us to adopt a chiral EFT Hamiltonian here and in the following section on neutron drops in an external trap. We also adopt the similarity renormalization group (SRG) approach [32–37]
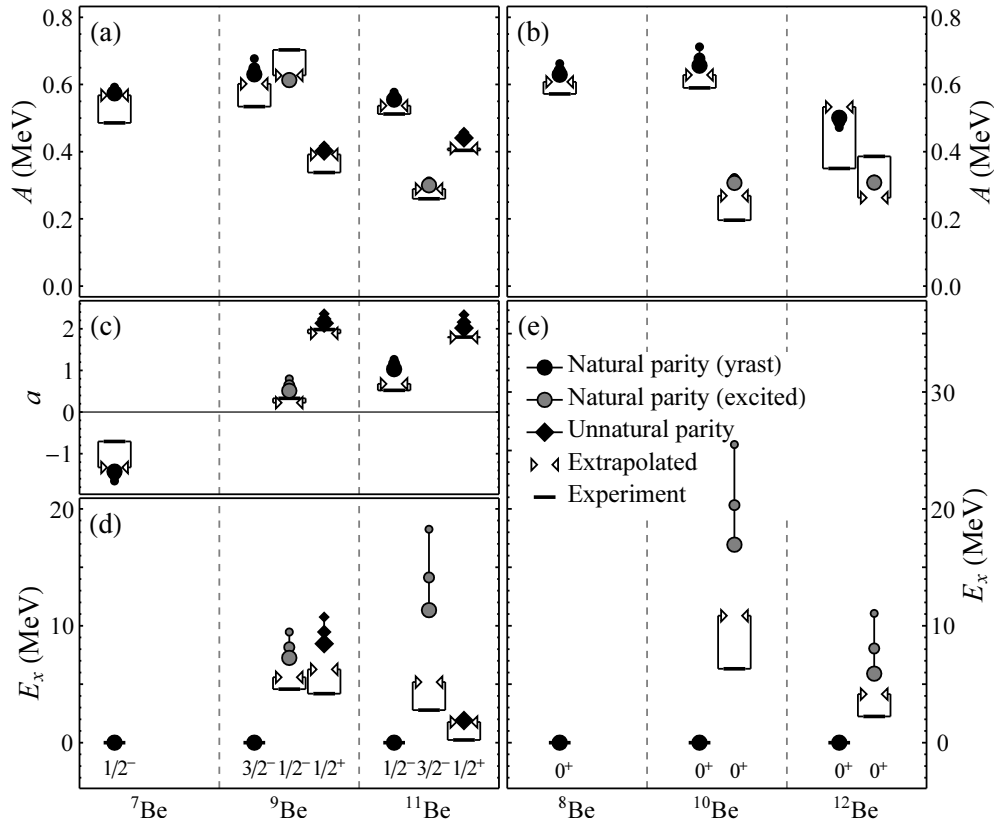
Figure 1: Rotational parameters A, a and E_x [defined relative to the yrast band as $E_x \equiv E_0 - E_{0,\mathrm{yrast}}$ — see Eq. (1)] for ground and excited bands of the Be isotopes (adapted from Ref [25]). Brackets highlight the difference between the parameters determined from experimental data (horizontal bars) and those extracted from NCFC calculations with extrapolation (parallel triangles) to the infinite matrix limit. Solid symbols connected by solid lines indicate the finite matrix results as a function of increasing $N_{\max}$ with larger symbols for larger $N_{\max}$ values. $N_{\max}$ is defined as the maximum number of oscillator quanta in the HO configurations above the minimum for the nucleus under investigation. The minimum $N_{\max}$ is 0 for natural parity and 1 for unnatural parity. The results indicated in the solid symbols correspond to $6 \leq N_{\max} \leq 10$ for natural parity and $7 \leq N_{\max} \leq 11$ for unnatural parity.

that allows us to consistently evolve (soften) the Hamiltonian and other operators, including $3N$ interactions [38–40].

We select the example of the spectroscopy of ^{12}C to illustrate the recent progress. In so doing, it is important to note that additional progress in achieving larger basis spaces is needed before we can realistically address cluster model states in light nuclei such as the celebrated "Hoyle state", a 0^+ state at 7.654 MeV of excitation energy in ^{12}C.

The theoretical excitation spectra are presented in Fig. 2 for the two highest $N_{\max}$ values currently achievable and are compared with experiment. For the negative parity states, we elect to show excitation energies relative to the lowest state of that parity whose experimental energy is 9.641 MeV above the ground state. The trends with increasing $N_{\max}$ (see the trends for additional observables in Ref. [41]) suggest convergence is sufficient to draw important conclusions regarding the underlying interaction. In particular, we note that the shifts from including the initial $3N$ interaction are substantial. In most cases, these shifts improve agreement between theory and
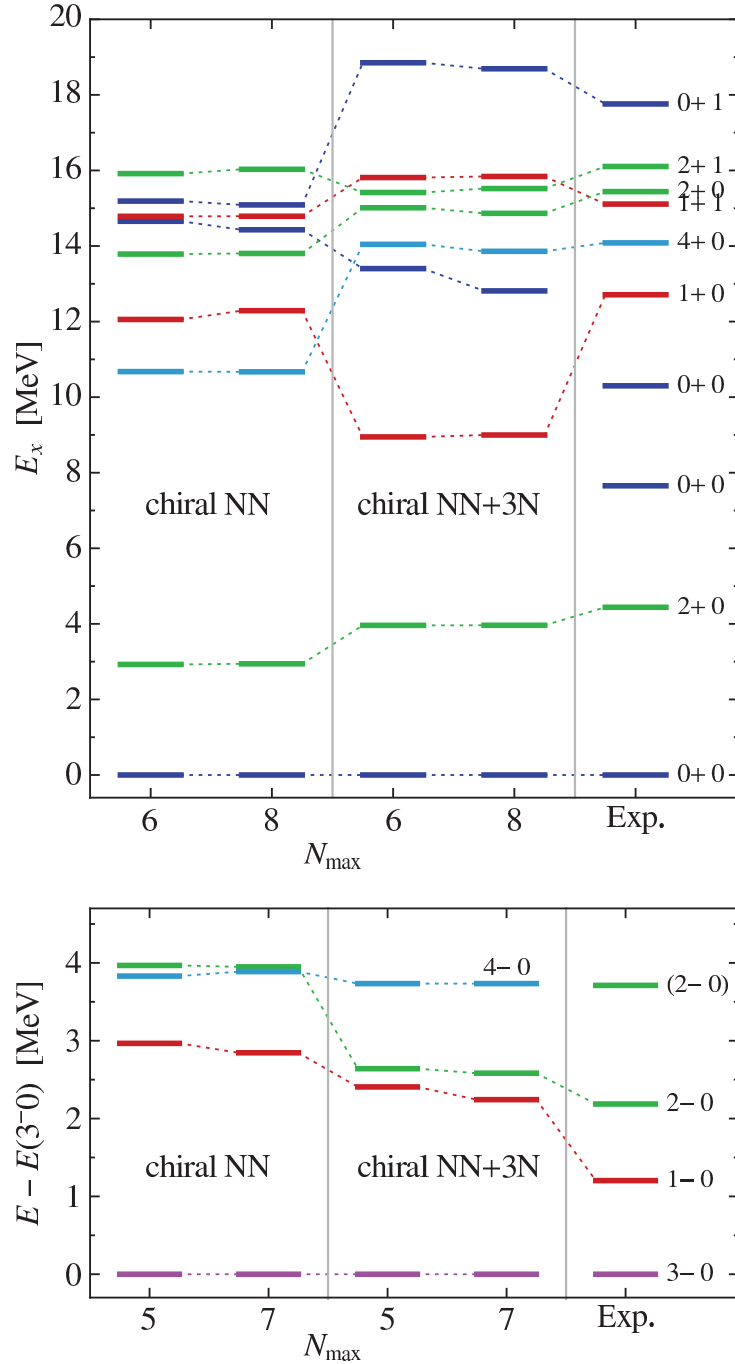
Figure 2: Theoretical and experimental excitation spectra of ^{12}C for both positive parity (top panel) and negative parity (bottom panel) states for two different values of N_{max} at $\hbar\Omega = 20$ MeV (adapted from Ref. [41]). The columns labelled "chiral NN" include the $3N$F induced by SRG while the sub panels labelled "chiral $NN + 3N$" include the initial $NN + 3N$F evolved by SRG together with NN. The SRG evolution parameter is $\lambda = 2.0$ fm^{-1}. See Ref. [41] for additional details.

experiment. A notable exception is the $J^{\pi} = 1^{+}$, $T = 0$ positive parity state which shifts further from experiment when we include the initial $3N$ interaction.

From our results in ^{12}C, we conclude that we need further improvements in the chiral interactions. For example, we need to have NN and $3N$ interactions at the same

chiral order to be consistent. We also need to extend the chiral order of the interactions to N4LO and, possibly, to include the derived four-nucleon ($4N$) interactions.

4   Confined neutron drops with chiral Hamiltonians

There are many motivations for considering artificial pure neutron systems confined by an external trap.

- Gain insights into the properties of systems dominated by multi-neutron degrees of freedom such as unstable neutron-rich nuclei and neutron stars.

- Isolate selected isospin components of the NN ($T = 1$) and $3N$ ($T = 3/2$) interactions for detailed study.

- Inform the development of nuclear energy density functionals that may be tuned to reproduce *ab initio* calculations, complementing their tuning to experimental data.

The external trap is required since realistic interactions do not bind pure neutron systems, though they do produce net attraction when the systems are confined. The main foci are to observe differences among realistic interactions and to see if subshell closures are predicted. For example, one may investigate spin-orbit splitting as a function of the chosen interaction and as a function of the external field parameters.

Using the same realistic chiral $NN + 3N$ interactions as used in the previous section, we investigated [15,16] neutron drop systems in a 10 MeV HO trap. In Ref. [16] we compared the results with those from Green's Function Monte Carlo (GFMC) and auxiliary field diffusion Monte Carlo (AFDMC) [42,43] using the Argonne v_8' (AV8') NN interaction [44] and the Urbana IX (UIX) $3N$ interaction. We also compared with GFMC and AFDMC results using AV8' with the Illinois-7 (IL7) $3N$ interaction [44,45].

For the investigations in Ref. [16] we employed both NCFC and coupled cluster (CC) methods. By implementing CC, we were able to obtain results for larger neutron drop systems.

We found important dependences on the selected interactions as shown in Fig. 3 which should have an impact on phenomenological energy-density functionals that may be derived from them. Note in Fig. 3 that, with increasing N, the chiral predictions lie between results from different high-precision phenomenological interactions, i. e. between AV8$'$+UIX and AV8$'$+IL7. It will be very important to see the influences the results of these different interactions have on energy density functionals.

One also notices in Fig. 3 there are surprisingly weak contributions from the inclusion of the chiral $3N$ interaction. Based on systematic trends shown in previous neutron-drop investigations [42,43,46], with non-chiral interactions we anticipate these conclusions will persist over a range of HO well strengths. Additional investigations are in progress to confirm this hypothesis and to extend the results to higher neutron numbers.

5   Computational accelerators and decoupling transformations

Fundamental physics investigations with chiral $NN + 3N$ interactions require forefront computational techniques in order to efficiently utilize leadership computational facilities. Many of our efforts are aimed to develop new algorithms that exploit the recent advances in hardware and software. Here we describe one of those projects

that could only have been accomplished through our multidisciplinary team working in close collaboration.

This specific project focused on adapting our NCSM code, Many-Fermion Dynamics — nuclear (MFDn), for use with GPU accelerators on the supercomputer Titan at Oak Ridge National Lab. MFDn represents the input NN and $3N$ interactions in the "coupled-JT" basis with coupled angular momentum and isospin, exploiting rotational symmetry and isospin conservation to reduce memory requirements [26, 38, 40]. In one representative case, storing a $3N$ input interaction in the coupled-JT basis reduces the interaction file size from 33 GigaBytes (GB) to less than 0.5 GB. This method is crucial for pushing the boundaries of problem sizes that we can address, as the input interactions must be stored once per process; using the ideal process configuration on Titan, processes have access to 16 GB each. Such a reduction in memory usage, then, not only enables calculations with larger input interactions, which are required for larger model spaces, but also makes their memory footprints more manageable, leaving more room for the memory-limited NCSM calculation.

As a side-effect of this compression, as we construct the full many-nucleon Hamiltonian from the input NN and $3N$ interactions, we must perform basis transformations to extract input interaction matrix elements that our code can use directly. These basis transformations are both computationally intensive and amenable to parallelization; they are a natural fit for Titan's GPU accelerators. We have taken advantage of our multidisciplinary team of physicists, computer scientists, and applied mathemati-
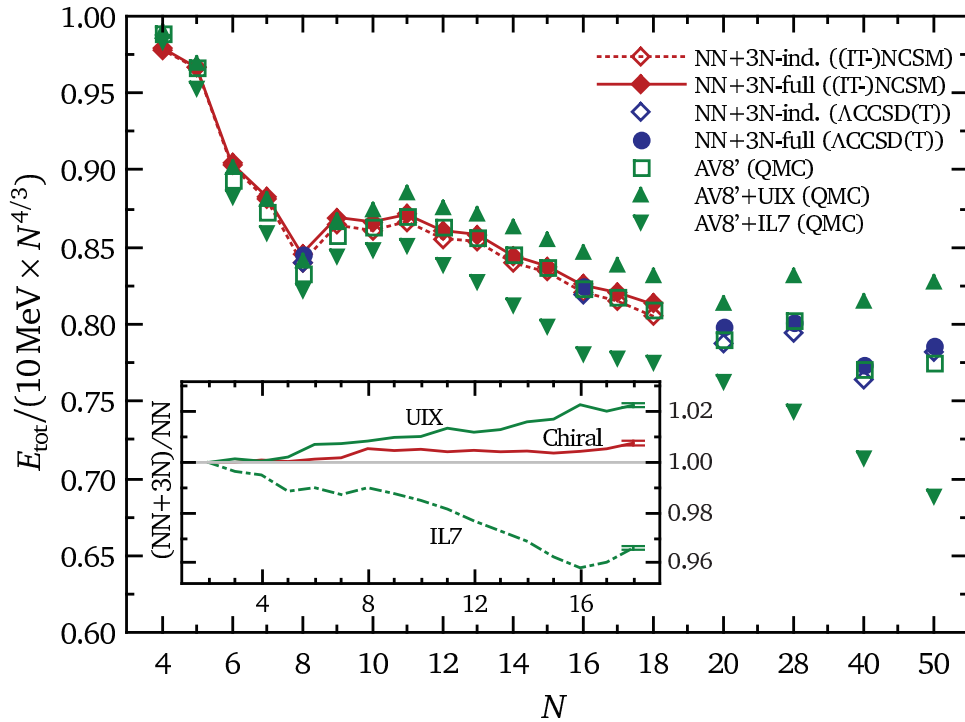

Figure 3: Comparison of ground state energies of systems with N neutrons trapped in a HO with strength 10 MeV. Solid red diamonds and blue dots signify results with $NN + 3N$ interactions derived from chiral effective field theory related to QCD. The inset displays the ratio of $NN + 3N$ to NN alone for the different interactions with the error indicated on the far right of each curve where it is maximum. The label indicates the many-body methods employed: (Importance-Truncated) No Core Shell Model ((IT-)NCSM); Coupled Cluster including Triples (ΛCCSD(T)); Quantum Monte Carlo (QMC). Figure adapted from Ref. [16].
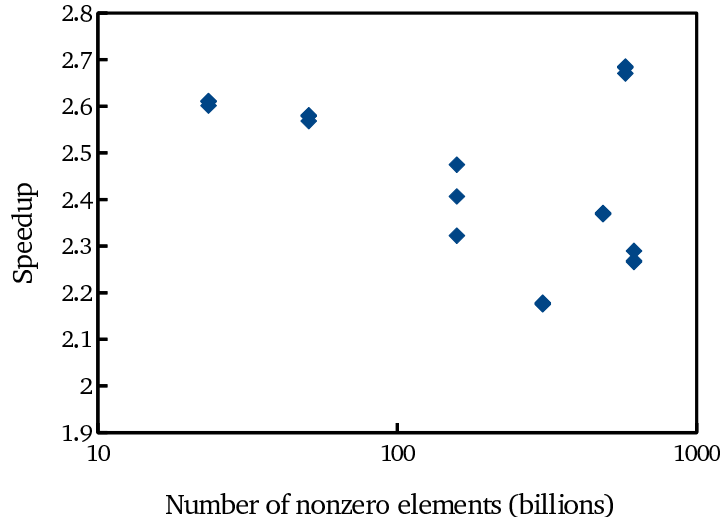
Figure 4: Speedup in the many-nucleon Hamiltonian construction stage due to implementation on GPU accelerators, graphed against the number of nonzero matrix elements in the Hamiltonian. There is no clear trend, but all speedups are in approximately the same region, indicating good weak scaling across this range of problem sizes. We graph matrix construction speedup here instead of overall speedup; overall speedup depends strongly on how long the matrix diagonalization takes, which is a function of the number of eigenstates required. Figure adapted from Ref. [15].

cians to port this section of our code to the GPU and optimize it [47]. Integrating the GPU-accelerated basis transformation into MFDn produces a speedup of 2.2x–2.7x in the many-nucleon Hamiltonian construction, as illustrated in Fig. 4, and a speedup of 1.2x–1.4x in the full calculation, with some variation depending on the particular problem chosen [15].

6   Overlapping communications and calculations

Our configuration interaction (CI) approach to the nuclear many-body problem results in a large sparse matrix eigenvalue problem with a symmetric real Hamiltonian matrix. This presents major technical challenges and is widely recognized as "computationally hard." One of the popular methods for obtaining the low-lying eigenvalues and eigenvectors is the Lanczos algorithm that we have implemented in MFDn. As the problem size increases with either increasing basis spaces or with the inclusion of $3N$ interactions, we face the challenge of communication costs rising with the increased numbers of nodes used in the calculations. The increase in nodes is driven by memory requirements as mentioned in the previous section.

In order to reduce communication costs, we developed an efficient mapping of the eigensolver onto the available hardware with a "topology-aware" mapping algorithm [13, 17]. We also developed an improved Lanczos algorithm that overlaps communications with calculations [14, 17].

For the challenge of efficiently overlapping communications with calculations, we worked with a hybrid MPI-OpenMP implementation and delegated one or a few threads to perform inter-process communication tasks, while the remaining threads carried out the multi-threaded computational tasks. In our algorithm, we also implemented a dynamical scheduling of the computations among the threads for the sparse matrix-vector multiplication (SpMV) so that, once a communication thread completes that task, it can participate in the multi-threaded computations.
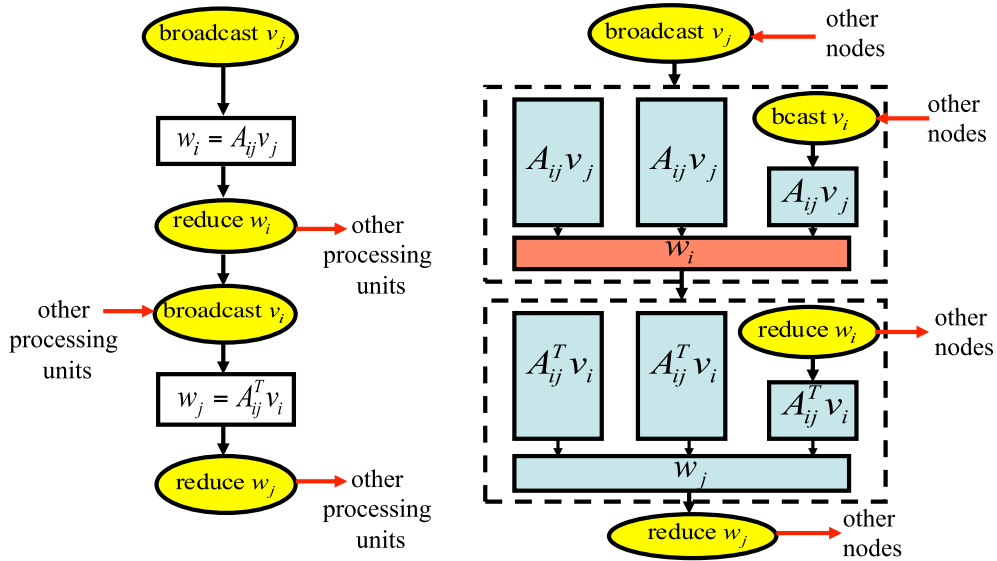
Figure 5: Comparison of SpMV and communication methods for an iteration of the Lanczos algorithm carried out by the majority of the processing units, the ones that store the off-diagonal blocks of the Hamiltonian matrix. The left subfigure displays a traditional sequential process that may be implemented with MPI. The right subfigure presents our algorithm suitable for hybrid MPI-OpenMP. Yellow ovals depict communication and rectangles depict computation. The red rectangle indicates where we require thread synchronization which incurs a small additional cost. The figure is adopted from Refs. [14, 17].

In Fig. 5 we compare a straightforward SpMV implementation using sequential steps (left subfigure) with our algorithm (right subfigure). By mapping MPI processes in a balanced column-major order as well as developing and implementing our algorithm to overlap communications and calculations, we achieved over 80% parallel efficiency through reduction in communication overhead during the Lanczos iteration process. This includes both the SpMV and orthogonalization steps that occur in each iteration. We also found major improvements in the scalability of the eigensolver especially after adopting our topology-aware mapping algorithm. Since SpMV and vector-vector multiplication of these types are common to many other iterative methods, we believe our achievements have a wide range of applicability.

7 Future prospects

Most of our applications have focused on light nuclei with atomic number $A \leq 16$ where our theoretical many-body methods have achieved successes with leadership class facilities. However, the frontiers of our field include applications to heavier nuclei and utilizing new and improved interactions from chiral effective field theory. At the same time, we aim to evaluate observables with increasing sophistication using their operators also derived within chiral effective field theory. We mention the example of neutrinoless double beta decay as one exciting example of frontier research with *ab initio* computational nuclear theory.

We therefore face the dual challenge of advancing the underlying theory at the same time as advancing the algorithms to keep pace with the growth in the size and complexity of leadership class computers. Recent history in these efforts, with the substantial support of the funding agencies, indicates we are experiencing a "Double

Moore's Law" rate of improvement — i. e. Moore's Law for hardware improvements and a simultaneous Moore's Law improvement in the algorithms/software. We need continued support for multi-disciplinary collaborations and growth in leadership class facilities in order to achieve the full discovery potential of computational nuclear physics.

8   Acknowledgements

References

[1] P. Navrátil, J. P. Vary and B. R. Barrett, Phys. Rev. Lett. **84**, 5728 (2000).

[2] P. Navrátil, J. P. Vary and B. R. Barrett, Phys. Rev. C **62**, 054311 (2000).

[3] P. Navrátil, V. G. Gueorguiev, J. P. Vary, W. E. Ormand and A. Nogga, Phys. Rev. Lett. **99**, 042501 (2007).

[4] P. Maris, J. P. Vary, A. M. Shirokov, Phys. Rev. C **79**, 014308 (2009); P. Maris, A. M. Shirokov and J. P. Vary, Phys. Rev. C **81**, 021301(R) (2010).

[5] B. R. Barrett, P. Navrátil and J. P. Vary, Progr. Part. Nucl. Phys. **69**, 131 (2013) and references therein.

[6] P. Maris and J. P. Vary, Int. J. Mod. Phys. E **22**, 1330016 (2013).

[7] A. M. Shirokov, V. A. Kulikov, P. Maris and J. P. Vary, in *Nucleon-Nucleon and Three-Nucleon Interactions*, eds. L. D. Blokhintsev and I. I. Strakovsky. Nova Science, Hauppauge, NY, 2014, p. 231, http://www.novapublishers.com/catalog/product_info.php?products_id=49997.

[8] P. Sternberg, E. G. Ng, C. Yang, P. Maris, J. P. Vary, M. Sosonkina and H. V. Le, in *Proc. 2008 ACM/IEEE Conf. on Supercomputing, Austin, November 15–21, 2008*. IEEE Press, Piscataway, NJ, 2008, p. 15:1.

[9] J. P. Vary, P. Maris, E. Ng, C. Yang and M. Sosonkina, J. Phys. Conf. Ser. **180**, 012083 (2009), arXiv:0907.0209 [nucl-th] (2009).

[10] P. Maris, M. Sosonkina, J. P. Vary, E. G. Ng and C. Yang, Proc. Comput. Sci. **1**, 97 (2010).

[11] H. M. Aktulga, C. Yang, E. G. Ng, P. Maris and J. P. Vary, in *Proc. 2011 Int. Conf. on High Performance Computing and Simulation (HPCS 2011), July 4 – July 8, 2011, Istanbul, Turkey.* IEEE Press, 2011, p. 176.

[12] P. Maris, H. M. Aktulga, M. A. Caprio, Ü. Çatalyürek, E. G. Ng, D. Oryspayev, H. Potter, E. Saule, M. Sosonkina, J. P. Vary, C. Yang and Z. Zhou, J. Phys. Conf. Ser. **403**, 012019 (2012).

[13] H. M. Aktulga, C. Yang, E. N. Ng, P. Maris and J. P. Vary, in *Euro-Par*, eds. C. Kaklamanis, T. S. Papatheodorou and P. G. Spirakis. Lecture Notes Comput. Sci. **7484**, 830 (2012).

[14] H. M. Aktulga, C. Yang, E. N. Ng, P. Maris and J. P. Vary, Concurrency Computat.: Pract. Exper. **26**, 2631 (2013).

[15] H. Potter, D. Oryspayev, P. Maris, M. Sosonkina, J. Vary, S. Binder, A. Calci, J. Langhammer, R Roth, Ü. Çatalyürek and E. Saule, in *Proc. Int. Conf. Nucl. Theor. Supercomputing Era (NTSE-2013), Ames, IA, USA, May 13–17, 2013*, eds. A. M. Shirokov and A. I. Mazur. Pacific National University, Khabarovsk, Russia, 2014, p. 263, http://ntse-2013.khb.ru/Proc/Sosonkina.pdf.

[16] H. D. Potter, S. Fischer, P. Maris, J. P. Vary, S. Binder, A. Calci, J. Langhammer and R. Roth, Phys. Lett. B **739**, 445 (2014).

[17] C. Yang, H. M. Aktulga, P. Maris, E. Ng and J. Vary, in *Proc. Int. Conf. Nucl. Theor. Supercomputing Era (NTSE-2013), Ames, IA, USA, May 13–17, 2013*, eds. A. M. Shirokov and A. I. Mazur. Pacific National University, Khabarovsk, Russia, 2014, p. 272, http://ntse-2013.khb.ru/Proc/Yang.pdf.

[18] T. Dytrych, K. D. Launey, J. P. Draayer, P. Maris, J. P. Vary, D. Langr and T. Oberhuber, *to be published in Proc. Int. Conf. Nucl. Theor. Supercomputing Era (NTSE-2014), Khabarovsk, Russia, June 23–27, 2014. Eds. A. M. Shirokov and A. I. Mazur. Pacific National University, Khabarovsk, Russia, 2015*, http://www.ntse-2014.khb.ru/Proc/.

[19] T. Abe, P. Maris, T. Otsuka, N. Shimizu, Y. Utsuno and J. P. Vary, *to be published in Proc. Int. Conf. Nucl. Theor. Supercomputing Era (NTSE-2014), Khabarovsk, Russia, June 23–27, 2014. Eds. A. M. Shirokov and A. I. Mazur. Pacific National University, Khabarovsk, Russia, 2015*, http://www.ntse-2014.khb.ru/Proc/.

[20] A.M. Shirokov *et al.*, *to be published in Proc. Int. Conf. Nucl. Theor. Supercomputing Era (NTSE-2014), Khabarovsk, Russia, June 23–27, 2014. Eds. A. M. Shirokov and A. I. Mazur. Pacific National University, Khabarovsk, Russia, 2015*, http://www.ntse-2014.khb.ru/Proc/.

[21] A. I. Mazur, A. M. Shirokov, I. A. Mazur, J. P. Vary and P. Maris, *to be published in Proc. Int. Conf. Nucl. Theor. Supercomputing Era (NTSE-2014), Khabarovsk, Russia, June 23–27, 2014. Eds. A. M. Shirokov and A. I. Mazur. Pacific National University, Khabarovsk, Russia, 2015*, http://www.ntse-2014.khb.ru/Proc/.

[22] T. Dytrych, K. D. Launey, J. P. Draayer, P. Maris, J. P. Vary, E. Saule, U. Catalyurek and M. Sosonkina, D. Langr and M. A. Caprio, Phys. Rev. Lett. **111**, 252501 (2013).

[23] M. A. Caprio, P. Maris and J. P. Vary, Phys. Lett. B **719**, 179 (2013).

[24] P. Maris, M. A. Caprio and J. P. Vary, Phys. Rev. C **91**, 014310 (2015).

[25] M. A. Caprio, P. Maris, J. P. Vary and R. Smith, Rom. J. Phys. **60**, 738 (2015), arXiv:1502.01083 [nucl-th] (2015).

[26] P. Maris, H. M. Aktulga, S. Binder, A. Calci, Ü. V. Çatalyürek, J. Langhammer, E. Ng, E. Saule, R. Roth, J. P. Vary and C. Yang, J. Phys. Conf. Ser. **454**, 012063 (2013).

[27] A. M. Shirokov, J. P. Vary, A. I. Mazur, S. A. Zaytsev and T. A. Weber, Phys. Lett. B **621**, 96 (2005).

[28] A. M. Shirokov, J. P. Vary, A. I. Mazur and T. A. Weber, Phys. Lett. B **644**, 33 (2007); fortran subroutines to generate the JISP16 interaction in the HO basis are available at http://nuclear.physics.iastate.edu.

[29] M. A. Caprio, P. Maris, J. P. Vary and R. Smith, Int. J. Mod. Phys. E *invited review paper, submitted*.

[30] E. Epelbaum, H.-W. Hammer and U.-G. Meißner, Rev. Mod. Phys. **81**, 1773 (2009).

[31] R. Machleidt and D. R. Entem, Phys. Rep. **503**, 1 (2011).

[32] S. D. Glazek and K. G. Wilson, Phys. Rev. D **48**, 5863 (1993).

[33] F. Wegner, Ann. Phys. **506**, 77 (1994).

[34] S. K. Bogner, R. J. Furnstahl, P. Maris, R. J. Perry, A. Schwenk and J. P. Vary, Nucl. Phys. A **801**, 21 (2008).

[35] H. Hergert and R. Roth, Phys. Rev. C **75**, 051001 (2007).

[36] S. K. Bogner, R. J. Furnstahl and A. Schwenk, Progr. Part. Nucl. Phys. **65**, 94 (2010).

[37] R. Furnstahl, Nucl. Phys. Proc. Suppl. **228**, 139 (2012).

[38] R. Roth, J. Langhammer, A. Calci, S. Binder and P. Navrátil, Phys. Rev. Lett. **107**, 072501 (2011).

[39] E. D. Jurgenson, P. Navrátil and R. J. Furnstahl, Phys. Rev. Lett. **103**, 082501 (2009).

[40] R. Roth, A. Calci, J. Langhammer and S. Binder, Phys. Rev. C **90**, 024325 (2014).

[41] P. Maris, J. P. Vary, A. Calci, J. Langhammer, S. Binder and R. Roth, Phys. Rev. C **90**, 014314 (2014).

[42] S. Gandolfi, J. Carlson and S. C. Pieper, Phys. Rev. Lett. **106**, 012501 (2011).

[43] P. Maris, J. P. Vary, S. Gandolfi, J. Carlson and S. C. Pieper, Phys. Rev. C **87**, 054318 (2013).

[44] B. S. Pudliner, V. R. Pandharipande, J. Carlson, S. C. Pieper and R. B. Wiringa, Phys. Rev. C **56**, 1720 (1997).

[45] S. C. Pieper, AIP Conf. Proc. **1011**, 143 (2008).

[46] S. Bogner, R. Furnstahl, H. Hergert, M. Kortelainen, P. Maris, M. Stoitsov and J. P. Vary Phys. Rev. C **84**, 044306 (2011).

[47] D. Oryspayev, H. Potter, P. Maris, M. Sosonkina, J. P. Vary, S. Binder, A. Calci, J. Langhammer and R. Roth, in *Proc. IEEE 27th Int. Parallel and Distrib. Processing Symp. Workshops & PhD Forum, Boston, MA, USA, 20–24 May, 2013.* 2013, p. 1365.